Food Chemistry 290 (2019) 95–100

Contents lists available at ScienceDirect

Food Chemistry

journal homepage: www.elsevier.com/locate/foodchem

The ultra-sensitive visual biosensor based on thermostatic triple step functional nucleic acid cascade amplification for detecting Zn^{2+}

ShuTing Li[a], GuiShan Li[a], ZaiHui Du[a], LongJiao Zhu[a], JingJing Tian[a], YunBo Luo[a,b], KunLun Huang[a,b], WenTao Xu[a,b,*]

[a] Beijing Advanced Innovation Center for Food Nutrition and Human Health, College of Food Science & Nutritional Engineering, China Agricultural University, Beijing 100083, China

[b] Beijing Laboratory for Food Quality and Safety, College of Food Science and Nutritional Engineering, China Agricultural University, Beijing 100083, China

ARTICLE INFO

Keywords:
Zn^{2+} ions
Functional nucleic acids
Thermostatic cascade amplification
Biosensor
Visual detection

ABSTRACT

Here, we present an ultra-sensitive visual biosensor based on thermostatic triple step functional nucleic acid cascade amplification for detecting Zn^{2+}. A Zn^{2+}-assisted cDNAzyme assay is conducted and the Zn^{2+} is successfully converted into nucleic acids to achieve the first circular amplification within 1 h. The cleavage products prompted Hybridization Chain Reaction (HCR), forming multiple DNA nanowire structures with branched chains. And the Strand Displacement Amplification (SDA) were further empowered by the HCR products with the addition of the amplification enzyme and the endonuclease. In just 80 min, the second and third-order signal amplifications are reached. With the addition of Hemin and chromogenic substrates, the visual signal output is achieved in 15 min based on the large amount of G-quadruplex (G4) DNAzymes. This biosensor can detect levels as low as 1.075 pM Zn^{2+}, showing a good linear range within 10 pM–100 nM. It shows considerable potential for the Zn^{2+} quantitative detection.

1. Introduction

Zn^{2+} is an essential trace element found in the human body, and plays a significant role in several physiological processes. Zn^{2+} is mainly ingested through food and water. The lack or excess thereof will affect general human health. Diseases such as Parkinson's, Alzheimer's and strokes are linked to abnormal levels of Zn^{2+} (Huang, 1997). In 2007 Pagani, Villarreal, Capdevila, and Atrian (2007) reported that the toxicity caused by excessive Zn^{2+} levels in the body could lead to increased cell viability. Therefore, it is vital to develop a technique for the accurate detection of Zn^{2+} in actual samples.

Traditional detection methods of Zn^{2+} include inductively coupled plasma emission spectrometry (ICP-AES) (Zhou, Xin, & Pu, 2012), inductively coupled plasma mass spectrometry (ICP-MS) (Jackson, Harper, Smith, & Flinn, 2006), atomic absorption spectrometry (AAS) (Soylak, Yilmaz, Ghaedi, & Montazerozohori, 2011), and more. Although these methods promote high sensitivity and specificity (Townsend, Miller, Mclean, & Aldous, 1998), they are highly dependent on precision instruments, and both the pre-processing and measurement processes of sample detection are cumbersome. Furthermore, the conditions involving the installation environment and maintenance requirements of instruments and equipment are demanding, and trained experts are necessary to operate these specialized tools. Additionally, these methods are unsuitable for rapid detection.

In recent years, along with the rapid development of molecular biotechnology, nucleic acid molecules with specific biological functions such as cDNAzymes and metal ion aptamers (Aptamers) have gradually made an appearance. Thus far, the known DNAzymes include Zn^{2+}, Cu^{2+}, Pb^{2+}, and Hg^{2+} dependent DNAzymes (Liu, Cao, & Lu, 2009; Zhu & Zhang, 2014). Most DNAzymes catalyze with the assistance of metal cofactors, some of which are highly selective and efficient. In addition, DNAzymes are remarkably stable and low in cost (Tian & Yi, 2012). These exceptional properties allow for the widespread utilization of DNAzymes in biosensors such as fluorescent biosensors (Wu, Khaing Oo, & Fan, 2010; Yin, Zuo, Huo, Zhong, & Ye, 2010), colorimetric biosensors (Huang et al., 2018; Bin Cheng Yin, Ye, Tan, Wang, & Xie, 2009), and electrochemical biosensors (Shen et al., 2008; Yang, Dou, Yuan, & Xiang, 2016).

HCR is a new type of in-vitro nucleic acid isothermal amplification technology, proposed by the Dirks team in 2004 (Dirks, Pierce, & Mayo, 2004). This method requires no enzymes or temperature changes, and two types of nucleic acid hairpins designed to contain energy. The presence of the nucleic acid stimulates the hairpins to open alternately. This process continues until all the hairpins in the buffer solution are exhausted. An extended DNA nanowire containing incisions is produced

* Corresponding author at: Beijing Advanced Innovation Center for Food Nutrition and Human Health, College of Food Science & Nutritional Engineering, China Agricultural University, Beijing 100083, China.
E-mail address: xuwentao@cau.edu.cn (W. Xu).

https://doi.org/10.1016/j.foodchem.2019.03.134
Received 17 November 2018; Received in revised form 21 March 2019; Accepted 25 March 2019
Available online 26 March 2019

by self-assembly, and signal amplification is ultimately achieved. HCR technology is currently widely applied in processes involving the detection of nucleic acid molecules (Huang et al., 2011), proteins (Zhang et al., 2012), cells (Choi, Love, Gong, Gierahn, & Love, 2011), ochratoxin A (OTA) (Wang, Dong, Liu, & Wang, 2015), and various additional small molecules (Ge et al., 2014; Li, Wang, Wang, & Wei, 2014). Furthermore, detection technology with HCR include advantages such as room temperature testing, simple operation, low experimental cost, high specificity, and excellent biocompatibility. Moreover, the nucleic acid hairpins and triggers lend themselves to easy modification. Although studies exist involving the application of HCR technology to locate heavy metal ions such as Pb^{2+} (Zhuang et al., 2013), and Hg^{2+} (Huang, Gao, Jia, Kim, & Li, 2014), specific research regarding the detection of Zn^{2+} ions is minimal.

In 1992, Walker et al. from the Becton Dickinson research center in the United States described an in-vitro isothermal amplification method known as SDA. This technique is assisted by nicking enzyme, which is activated by specific primers and produces single-stranded DNA products (Walker et al., 1992). During the SDA process, the specific sequences are usually modified at both ends of the target sequences by the researchers to enable restriction endonuclease recognition. During this reaction, the endonuclease cleaves the ends of the target sequences at its recognition sites, enabling the DNA polymerase to extend the 3′ end gap and replace a DNA strand. A substantial amount of single-stranded DNA is formed following the circulation amplification, leading to the signal amplification of the targets. Furthermore, this technology displays substantial beneficial characteristics such as uncomplicated operation, reduced testing time, high sensitivity and specificity, and excellent compatibility (Du, Zhu, & Kong, 2016). In recent years, researchers have shown great interest in using SDA technology to achieve the signal conversion of targets. For example, Zhou team used SDA technology to generate a large number of Mg^{2+}-dependent cDNAzyme sequences, and realized the quantitative fluorescence detection of target microRNA-21 (Yin et al., 2017).

As a specific functional nucleic acid, a Guanine-rich sequence can form a coordination complex (G4 DNAzyme) when combined with Hemin which displays peroxidase-like catalytic activity. The catalytic activity of this combination is approximately ten times higher than Hemin alone, significantly improving the catalytic performance of Hemin itself (Travascio, Li, & Sen, 1998). G4 DNAzyme has been extensively employed in the catalyzation of H_2O_2 regulated redox reactions. For example, it was used to catalyze the oxidation of colorless diammonium 2,2′-azino-bis(3-ethylbenzothiazoline-6-sulfonate) ($ABTS^{2-}$) by H_2O_2 to produce the green free radical $ABTS^{\cdot -}$ (Xiao et al., 2005). This color rendering principle is simple, fast and does not require enzyme catalysis. Therefore, it has attracted the attention of several researchers and has been extensively applied in the construction of colorimetric biosensors (Elbaz, Moshe, Shlyahovsky, & Willner, 2010; Teller, Shimron, & Willner, 2009).

Given the necessity for a quantitative detection technique with good sensitivity and specificity, a visual biosensor was constructed based on thermostatic triple step functional nucleic acid cascade amplification to achieve the rapid visual detection of Zn^{2+}. This structure was established by inserting the HCR trigger sequences into the substrate chains (S-HCR) of the Zn^{2+}-dependent cDNAzyme. Both the complementary Guanine-rich sequences and the restriction site sequences were inserted into the 5′ end of the hairpins. Consequently, the S-HCR were cleaved following the specific recognition of Zn^{2+} by the cDNAzymes. The products obtained from the cleavage process prompted the HCR reactions to form DNA nanowire structures with branched chains. The products generated by the HCR further empowered the multiple SDA reactions, with the addition of the amplification enzyme and endonuclease. Therefore, an abundance of Guanine-rich sequences were formed and combined with Hemin to prompt the production of multiple G4 DNAzymes. Following the addition of the chromogenic substrates, the G4 DNAzymes efficiently catalyzed H_2O_2 to oxidize the colorless $ABTS^{2-}$ into the green free radical $ABTS^{-}$, achieving the visual detection of Zn^{2+}.

In a word, this study establishes a universal thermostatic amplification Zn^{2+} recognition system with high sensitivity and specificity. And it does not require large instruments, is not complicated to operate, and is visually detectable by the naked eye. Moreover, real sample was analyzed, showing that this strategy we proposed is reliable and has great application potential in monitoring human health.

2. Materials and methods

2.1. Materials

All oligonucleotide sequences are listed in Table S-1 and were synthesized by Ningbo Kangbei Biochemical Co. Ltd (Zhejiang, China). NaCl, KCl, $MgCl_2$, $ZnCl_2$, $CaCl_2$, $CuCl_2$, HgCl, $NiCl_2$, NaH_2PO_4, Na_2HPO_4, and Citric acid were purchased from the Sinopharm Pharmaceutical Co. Ltd (Beijing, China), and they were all analytically pure. H_2O_2 was purchased from the Lanyi Chemical Product Co. Ltd (Beijing, China). Tris(hydroxymethyl)aminomethane (Tris), ethylenediaminetetraacetic acid (EDTA), 4-hydroxyethylpiperazine ethyl sulfonic acid (HEPES), Hemin, dimethyl sulfoxide (DMSO), $ABTS^{2-}$, agarose and 2-(2-[4-(1,1,3,3-tetramethylbutyl)phenoxy]ethoxy)ethanol (Triton X-100) were purchased from Sigma (St. Louis, MO, USA). The Bst DNA polymerase and the Nt. Bst NBI nicking enzyme was purchased from New England BioLabs (USA), and the dNTP was purchased from the Takara Biotech Co. Ltd (Dalian, China). The DNA marker was purchased from the Tiangen Biotech Co. Ltd (Beijing, China).

2.2. Zn^{2+}-dependent cDNAzymes and S-HCR lysis and hybridization

The test tube containing the synthetic sequence powder was placed in a high-speed centrifuge (ACTGene, USA) at 13,400 × *g* for 10 min at 4 °C. The sample was subsequently removed, and the sequence powder was dissolved by adding ultrapure water to the tube. A dilution of 10 μM was obtained at 4 °C and set aside for later. A 100 μL of the S-HCR (10 μM) and a 100 μL of the catalytic enzyme chain (E-HCR) (10 μM) were added to 800 μL of cleavage buffer (300 mM NaCl, 40 mM HEPES, and pH 7.5). The mixture was heated at 95 °C for 5 min and gradually cooled to room temperature to obtain a 1 μM Zn^{2+}-dependent cDNAzyme solution (17 ES-HCR).

2.3. Zn^{2+} assisted DNAzyme cleavage assay and HCR reaction

To conduct the cleavage assay, a 30 μL quantity of cleavage buffer, 4 μL of 17 ES-HCR, and 2 μL of $ZnCl_2$ solution were mixed and incubated at 37 °C for 60 min. Subsequently, 2 μL of Y-H1 (10 μM) and 2 μL of Y-H2 (10 μM) were added to the reaction system and incubated at 37 °C for another 60 min for the HCR assay.

2.4. Agarose gel electrophoresis analysis

To identify whether the HCR reaction occurs or not, various HCR reaction mixtures were analyzed by agarose gel electrophoresis. HCR products were loaded onto 2 wt% agarose gel sample ports, and placed into the 1 × TAE running buffer at pH 8.0. The gel electrophoresis was performed at 130 V for 15 min. Following the electrophoresis process, an electropherogram was taken using the BioDoc-It imaging system (CA, USA).

2.5. SDA reaction

A 5 μL quantity of HCR products, 28.5 μL of water, 5 μL of Thermpol Buffer (10 ×), 5 μL of NEB 3.1 Buffer (10 ×), 5 μL of dNTP (2.5 mM), 0.5 μL of the Bst DNA polymerase, and 1 μL of the Nt. Bst NBI nicking enzyme were added to the reaction system described above. Amplification was conducted at 55 °C for 20 min, followed by an inactive period at 95 °C for 5 min. Subsequently, the mixture was stored at 4 °C for 5 min.

2.6. Color reaction and UV–visible absorption spectroscopy

A 66 μL quantity of enzyme activity buffer, 4 μL of Hemin (100 μM), and 10 μL of SDA products were mixed. The solution was incubated at 37 °C for 10 min to allow for the complete development of the G4 DNAzyme. Following this process, a 20 μL quantity of $ABTS^{2-}$ (3.6 mM) was added. Incubation proceeded at 37 °C for 4 min to obtain a color reaction. The absorbance of 385–450 nm was measured using a Multi-Mode Microplate Reader (Thermo Fisher Scientific, USA).

2.7. The calculation method of the LOD

According to the LOD calculation method created by the Vashist team (Vashist, Schneider, Lam, Hrapovic, & Luong, 2014), the LOD in this study was calculated as follows:

The ΔOD_{415nm} value corresponding to the LOD = the average value of the blank sample $\Delta OD_{415nm} - 3\sigma$ (σ represented the standard deviation of the lowest analytical concentration), after which the minimum detection concentration of the Zn^{2+} visual biosensor was derived from the standard curve.

2.8. The specificity of the sensor

To determine the specificity of the biosensor, the interfering metal ions including Mg^{2+}, Ca^{2+}, Cu^{2+}, Hg^{2+}, and Ni^{2+} were examined by comparing the ΔOD_{415nm} of different treatments. Solutions of all the tested ions were prepared at the same concentration of 10 μM and individually spiked into the detection system, while Zn^{2+} was at a concentration of 1 μM.

3. Results and discussion

3.1. The principle of the assay

The construction of the Zn^{2+} functional nucleic acid colorimetric biosensor based on triple step thermostatic cascade amplification is schematically illustrated in Scheme 1. The system features the following three main components. (A) This step refers to the Zn^{2+} assisted cDNAzyme assay. The S-HCR and the E-HCR were connected by the complementary bases. The cDNAzymes specifically recognized Zn^{2+} and its cleavage activity was stimulated to divide the S-HCR. At the appropriate temperature, Zn^{2+} can be circulated continuously, encouraging the cleavage of the S-HCR to achieve the first circular amplification. (B) HCR trigger sequences were inserted into the S-HCR of the Zn^{2+}-dependent cDNAzymes. Two types of hairpin DNA (Y-H1 and Y-H2) were added, instantly prompting an HCR reaction by the cleavage products. This reaction opened the hairpins to form DNA nanowire structures with branched chains resulting in second-order signal amplification. (C) Both the complementary Guanine-rich sequences and the restriction sites sequences were inserted into the 5′ end of the hairpins. Therefore, multiple SDA reactions were further empowered by the HCR products with the addition of the Bst DNA polymerase and the Nt. Bst NBI nicking enzyme. During the SDA reaction, a large amount of Guanine-rich sequences were produced to realize the third-order signal amplification. With the addition of Hemin, multiple G4 DNAzymes were formed displaying catalytic activity similar to that of peroxidase. Subsequently, the chromogenic substrates were added, and the G4 DNAzymes efficiently catalyzed H_2O_2 to oxidize the colorless $ABTS^{2-}$ to green free radical $ABTS^{-}$. The amount of target Zn^{2+} could be judged by the color depth, leading to the visual detection of Zn^{2+}.

3.2. HCR triggerability verification

In order to verify that the nucleic acid hairpins (Y-H1, Y-H2) designed in this study can trigger the HCR reaction well and be applied to the construction of biosensor, we analyzed it by agarose gel electrophoresis. As can be seen from Fig. 1, Compared with the control groups, Y-H1 and Y-H2 can better trigger the HCR reaction and form a distinct diffusion band. Therefore, they can be used in subsequent experiments.

3.3. Feasibility verification of the Zn^{2+} visual biosensor

Fluorescence measurement was used to investigate the feasibility of the strategy proposed in this study. As shown in Fig. 2, the absorbance of treatment 5 is significantly higher than that of the other treatment groups. The results indicate that the cleavage, as well as the HCR and SDA reactions, can only be achieved when the system contains all the assay reagents. This process generates a large number of Guanine-rich sequences that combine with Hemin to form G4 DNAzymes exhibiting high catalytic activity. This combination is ultimately highly efficient in catalyzing $ABTS^{2-}$ color development, resulting in a color that is significantly darker than that of other treatment groups. When the system contains all assay reagents excluding the target Zn^{2+}, low fluorescence intensity is exhibited (curve 4). Consequently, the S-HCR cannot be cleaved without Zn^{2+} which impedes both the HCR and SDA process. Therefore, the proposed strategy displays excellent feasibility.

3.4. Optimization of the system parameters

To achieve the best sensing performance, different experimental parameters such as the SDA amplification time, the concentration of the Bst DNA polymerase, the Nt. Bst NBI nicking enzyme and Hemin were optimized. Fig. 3(a) indicates that the absorbance value of the treatment group increases rapidly in conjunction with a high amplification time, reaching its peak after 20 min, followed by a steady decline. The result shows that the SDA reaction is extremely efficient and can rapidly consume dNTP to synthesize a large number of Guanine-rich sequences during a brief period of time. In conclusion, an amplification time of 20 min was selected as the optimal time for subsequent experiments.

Enzyme concentration dramatically affects reaction rates. Therefore, the concentration of both the Bst DNA polymerase and the Nt. Bst NBI nicking enzyme were optimized. Fig. 3(b) illustrates that the initial increase in the Bst DNA polymerase concentration causes the absorbance value to rise rapidly. The absorbance value is at its highest when the Bst. DNA polymerase concentration reaches 0.08 U/μL, before leveling out. These results indicate that under experimental conditions, the concentration of the Bst DNA polymerase is close to the saturation concentration when it is at 0.08 U/μL. After exceeding 0.08 U/μL, the concentration has little effect on continued color development. Therefore, 0.08 U/μL was chosen as the optimal Bst DNA polymerase concentration. Fig. 3(c) illustrates a rapid growth in the absorbance value with the increase of the Nt. Bst NBI nicking enzyme concentration, reaching a maximum level at 0.2 U/μL, and then declines rapidly. The reason may be that when the nicking enzyme concentration is around 0.2 U/μL, it can achieve the optimal cleavage and amplification ratio when combined with a 0.08 U/μL quantity of the Bst DNA polymerase. When the nicking enzyme concentration is too high, the cleavage rate exceeds the amplification rate, leading to the ineffective formation of the amplification products, and therefore reducing the final absorption value. A Nt. Bst NBI nicking enzyme concentration of 0.2 U/μL was considered optimal and was selected for subsequent experiments.

It is necessary for the Guanine-rich sequence to combine with Hemin to achieve optimal peroxidase-like activity. The specific levels of Hemin exert significant influence on the absorbance value and necessitated further exploration of its effect on the detection system. Fig. 3(d) shows that the absorbance value initially exhibits a gradual rise and then tends to stabilize in conjunction with an elevated Hemin concentration. This result illustrates that the saturation concentration of Hemin is approximately 4 μM. A quantity of 4 μM was chosen for utilization in further experimentation.

3.5. The sensitivity of the Zn^{2+} visual biosensor

Various concentrations of Zn^{2+} standard samples (0; 10 pM; 100 pM; 1 nM; 10 nM; 100 nM; 1 μM; and 10 μM, respectively) were

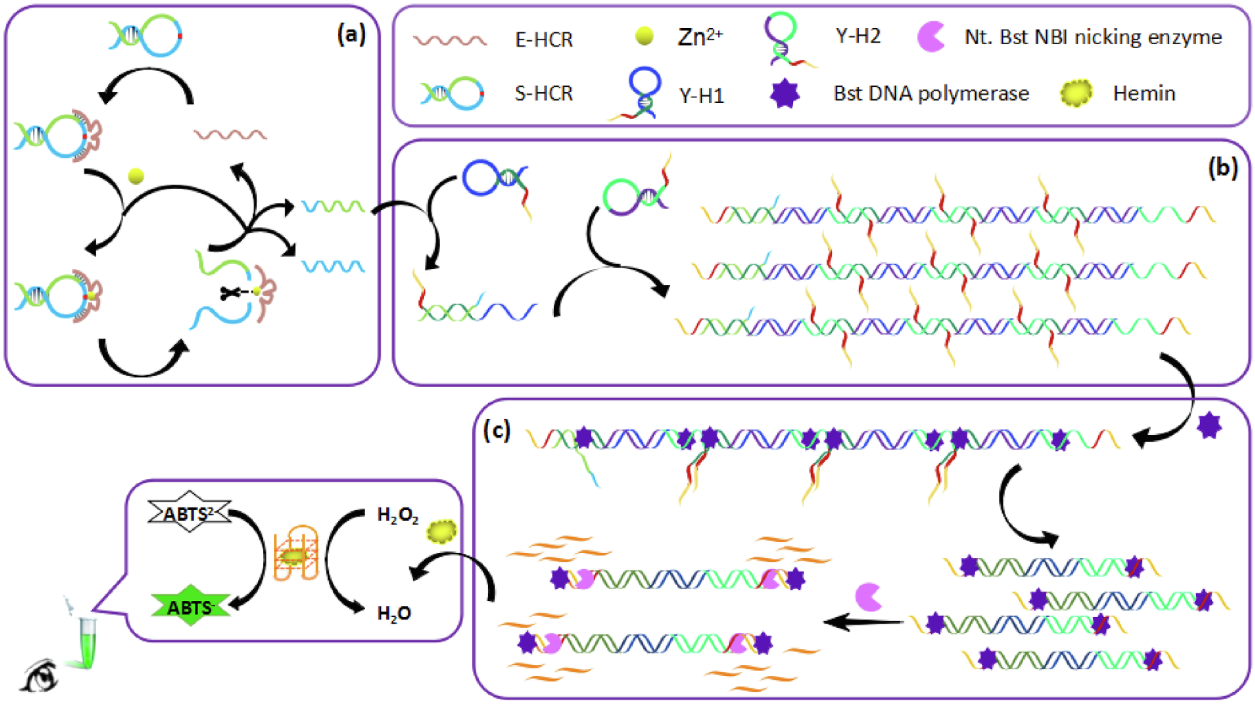

Scheme 1. The principle of the sensing system for Zn^{2+} detection based on Zn^{2+}-dependent cDNAzymes (a), HCR (b), and SDA (c) reactions.

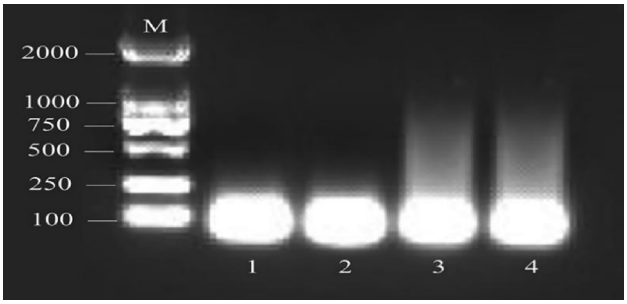

Fig. 1. Agarose gel electrophoresis of HCR trigger results. M: DNA Marker DL 2000; (1, 2): Y-H1 + Y-H2; (3, 4): trigger + Y-H1 + Y-H2. Conditions: $C_{trigger}$ = 100 nM, $C_{Y\text{-}H1}$: $C_{Y\text{-}H2}$ = 500 nM: 500 nM.

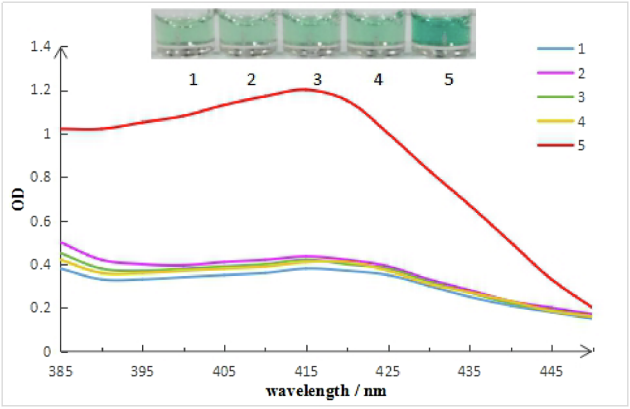

Fig. 2. Schematic of UV–visible absorption spectrum analysis. 1: cDNAzyme + SDA; 2: cDNAzyme + 10 μM Zn^{2+} + SDA; 3: Y-H1 + Y-H2 + SDA; 4: cDNAzyme + Y-H1 + Y-H2 + SDA; 5: cDNAzyme + 10 μM Zn^{2+} + Y-H1 + Y-H2 + SDA. The inset is a photograph of the corresponding system.

added to the detection system in an attempt to verify the analytical capability of the visual biosensor under optimal conditions with Zn^{2+} as the target. A UV–visible absorption spectroscopy with a wavelength range of 385–450 nm (interval of 5 nm) was performed following the completed reaction. As shown in Fig. 4(a), the absorption value increases when the concentration of the target Zn^{2+} is raised from 0 to 10 μM. Fig. 4(b) represents the standard curve. Under optimal conditions, the change in the absorbance value at the maximum absorption wavelength was found to exhibit a linear correlation to the logarithm of target Zn^{2+} concentrations from 10 pM to 100 nM. The linear equation is $y = 0.1411x - 0.0209$ with a linear correlation coefficient of 0.9968, and the LOD at 1.075 pM. The high sensitivity of the approach employed by this study is likely attributed to the three-step signal amplification reactions that include the Zn^{2+} assisted cDNAzyme assay, HCR, and SDA, as well as the background reduction of the unique hairpin type S-HCR.

The LOD of different Zn^{2+} biosensors were compared and the results are shown in Table S-2. The LOD of the Zn^{2+} visual biosensor created for this study reached the pM level, while the LOD of the comparison biosensors were as high as the nM level. Therefore, the LOD of this detection system is far lower than other biosensors. The Zn^{2+} visual biosensor established in this paper displays clear advantages relating to both high sensitivity and visualization. The difference in Zn^{2+} concentrations among varying samples can be distinguished by the naked eye, which is impossible to achieve with other methods. Therefore, the proposed strategy exhibits great promise as a useful tool for the quantitative detection of Zn^{2+}.

3.6. The specificity of the Zn^{2+} visual biosensor

The specificity of the Zn^{2+} visual biosensor was further verified as shown in Fig. 5. The change in absorbance value at 415 nm (ΔOD_{415nm}) of the Zn^{2+} treatment group is much higher than other metal ions. Moreover, the visible green color is darker, indicating that the specificity of the Zn^{2+} visual biosensor is excellent. This result may be attributed to the specificity of the Zn^{2+}-dependent cDNAzyme. When Zn^{2+} is added to the detection system, it can effectively catalyze the cleavage of the S-HCR by the cDNAzymes, further encouraging the HCR and SDA reactions. Furthermore, it is noteworthy to mention that the ΔOD_{415nm} of Ni^{2+} is highly negative, and is likely because it inhibited the activity of the Bst DNA polymerase or the Nt. Bst NBI nicking enzyme.

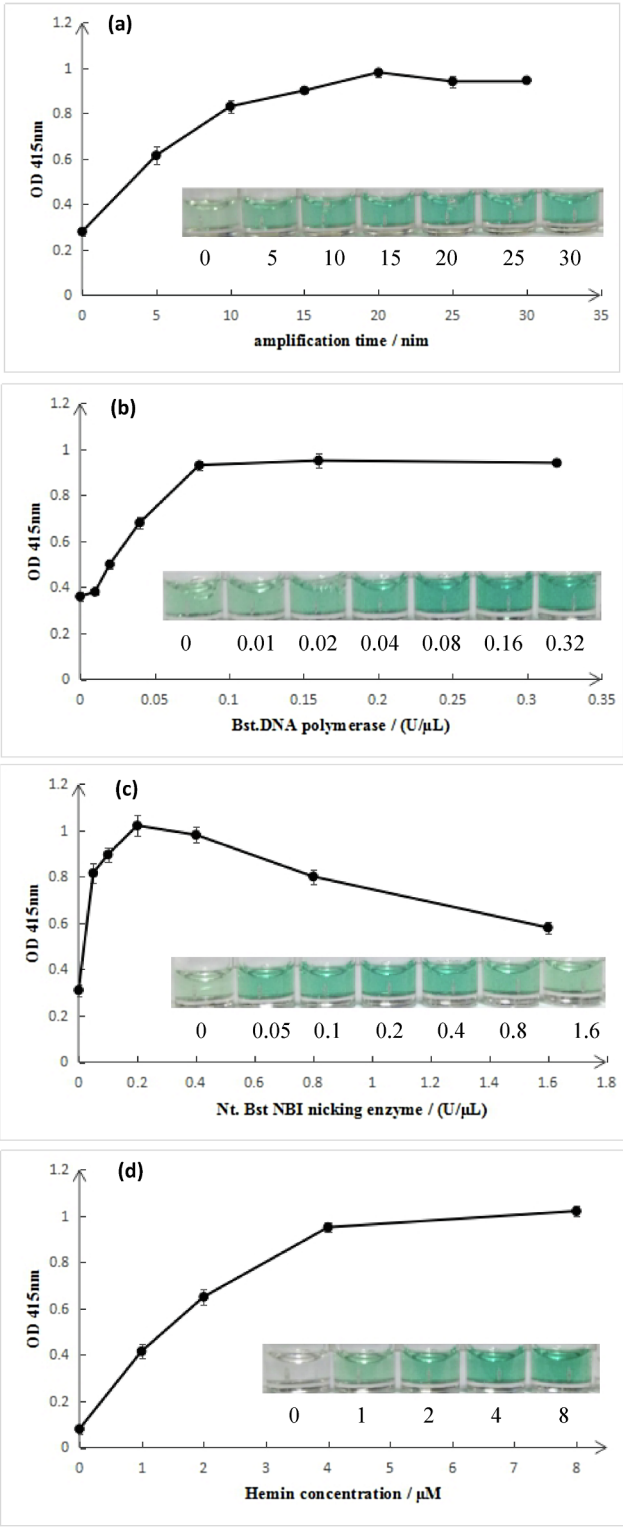

Fig. 3. The effect of SDA amplification time (a); the Bst DNA polymerase concentration (b); the Nt. Bst NBI nicking enzyme concentration (c); and the Hemin concentration (d). Each data point represents an average of three measurements (each error bar indicates the standard deviation). The inset is a photograph of the corresponding system. Conditions: $C_{Zn^{2+}}$ = 1 mM, $C_{17ES\text{-}HCR}$ = 100 nM, $C_{Y\text{-}H1}$: $C_{Y\text{-}H2}$ = 500 nM: 500 nM.

3.7. Real sample analysis of the Zn^{2+} visual biosensor

In order to investigate the detection ability of this method in real sample, the recovery experiment of Zn^{2+} was conducted by a standard addition method in human serum. Different concentrations of Zn^{2+} were spiked in human serum samples and then analyzed. 0.45 μm membrane filter was used to filter the human serum samples before the testing. The experimental results are shown in Table S-3, the recovery rate of Zn^{2+} in serum varied from 97.37% to 101.03%, and the relative standard deviation (RSD) was less than 2.26%. These results indicate that this Zn^{2+} visual quantitative sensing system has application potential in real samples.

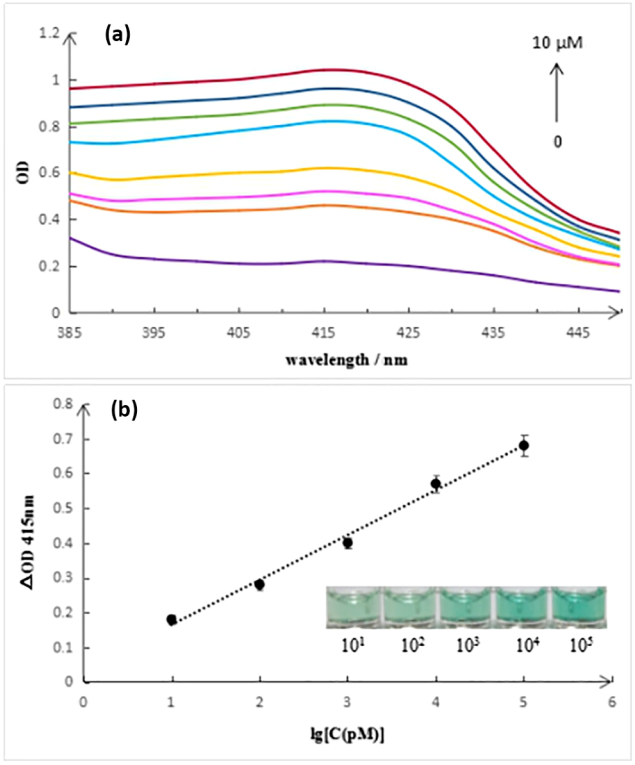

Fig. 4. (a) UV–visible absorption spectrum obtained in the proposed detection strategy for the detection of target Zn^{2+} with varying concentrations from 0 to 10 μM; (b) The calibration curve of the absorbance value changes at 415 nm as a function of the Logarithm of Zn^{2+} concentration (The inset is a photograph of the corresponding system). Each data point represents an average of three measurements (each error bar indicates the standard deviation). Conditions: $C_{17ES\text{-}HCR}$ = 100 nM, $C_{Y\text{-}H1}$: $C_{Y\text{-}H2}$ = 500 nM: 500 nM, $C_{Bst.DNA\ polymerase}$ = 0.08 U/μL, $C_{Nt.\ Bst\ NBI\ nicking\ enzyme}$ = 0.2 U/μL, C_{Himin} = 4 μM.

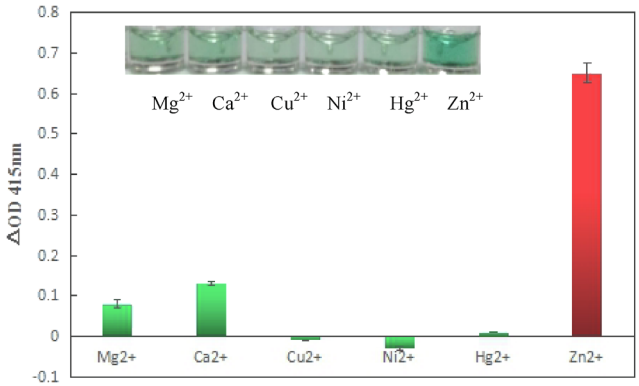

Fig. 5. Schematic of the specific experimental results. 1 μM Zn^{2+}, 10 μM Mg^{2+}, 10 μM Ca^{2+}, 10 μM Cu^{2+}, 10 μM Ni^{2+}, and 10 μM Hg^{2+} were used as the cleavage concentrations. The inset is a photograph of the corresponding system. Each data point represents an average of three measurements (each error bar indicates the standard deviation).

4. Conclusion

In conclusion, an ultra-sensitive visual biosensor was successfully constructed to detect Zn^{2+} ions. This biosensor was based on thermostatic triple-step functional nucleic acid cascade amplification. During this study, the HCR trigger sequences were inserted into the substrate chains of the Zn^{2+}-dependent cDNAzyme to avoid self-activation, which reduced the background value and improved the specificity. Furthermore, both the complementary Guanine-rich sequences and the restriction site sequences were inserted into the 5′ end of the two hairpins. Therefore, multiple SDA reactions were successfully empowered by the HCR products to generate a substantial amount of G4 DNAzyme. Consequently, both signal amplification and visual detection of Zn^{2+} were achieved. The sensitivity of the biosensor was significantly improved by the three-step thermostatic amplification process with a LOD as low as 1.075 pM. Moreover, the ultimate realization of Zn^{2+} visual detection does not require sophisticated signal output devices, and can be differentiated by the naked eye. Furthermore, this method is universal, and the detection of additional metal ions can be achieved by changing the specific cDNAzymes and substrate chains of the targets. In summary, this research established a Zn^{2+} visual biosensor that is simple and fast to operate, while maintaining high visibility. Additionally this biosensor displays exceptional sensitivity and specificity and provides a technical reference for the visual detection of trace Zn^{2+}.

Conflict of interest

The authors have read the policy on Conflicts of interest and declare no competing financial interests.

Acknowledgement

This work was supported by the National Grand Project of Science and Technology (2018ZX0801106B).

Notes

The authors declare no competing financial interests.

Appendix A. Supplementary data

The tables of the sequences of Zn^{2+}-dependent cDNAzymes and hairpins used in this work, the comparison of the LOD of different Zn^{2+} ion biosensors and Zn^{2+} analysis in real samples. Supplementary data to this article can be found online at https://doi.org/10.1016/j.foodchem.2019.03.134.

References

Choi, J., Love, K. R., Gong, Y., Gierahn, T. M., & Love, J. C. (2011). Immuno-hybridization chain reaction for enhancing detection of individual cytokine-secreting human peripheral mononuclear cells. *Analytical Chemistry, 83*(17), 6890.

Dirks, R. M., Pierce, N. A., & Mayo, S. L. (2004). Triggered amplification by hybridization chain reaction. *Proceedings of the National Academy of Sciences of the United States of America, 101*(43), 15275–15278.

Du, Y. C., Zhu, L. N., & Kong, D. M. (2016). Label-free thioflavin T/G-quadruplex-based real-time strand displacement amplification for biosensing applications. *Biosensors & Bioelectronics, 86*, 811–817.

Elbaz, J., Moshe, M., Shlyahovsky, B., & Willner, I. (2010). Cooperative multicomponent self-assembly of nucleic acid structures for the activation of DNAzyme cascades: A paradigm for DNA sensors and aptasensors. *Chemistry – A European Journal, 15*(14), 3411–3418.

Ge, J., Huang, Z. M., Xi, Q., Yu, R. Q., Jiang, J. H., & Chu, X. (2014). A novel graphene oxide based fluorescent nanosensing strategy with hybridization chain reaction signal amplification for highly sensitive biothiol detection. *Chemical Communications, 50*(80), 11879–11882.

Huang, C., Fan, X., Yuan, Q., Zhang, X., Hou, X., & Wu, P. (2018). Colorimetric determination of uranyl (UO22+) in seawater via DNAzyme-modulated photosensitization. *Talanta, 185*, 258–263.

Huang, E. P. (1997). Metal ions and synaptic transmission: Think zinc. *Proceedings of the National Academy of Sciences of the United States of America, 94*(25), 13386–13387.

Huang, J., Gao, X., Jia, J., Kim, J. K., & Li, Z. (2014). Graphene oxide-based amplified fluorescent biosensor for Hg(2+) detection through hybridization chain reactions. *Analytical chemistry, 86*(6), 3209.

Huang, J., Wu, Y., Chen, Y., Zhu, Z., Yang, X., Yang, C. J., ... Tan, W. (2011). Pyrene-excimer probes based on the hybridization chain reaction for the detection of nucleic acids in complex biological fluids. *Angewandte Chemie, 50*(2), 401–404.

Jackson, B., Harper, S., Smith, L., & Flinn, J. (2006). Elemental mapping and quantitative analysis of Cu, Zn, and Fe in rat brain sections by laser ablation ICP-MS. *Analytical & Bioanalytical Chemistry, 384*(4), 951–957.

Li, X., Wang, Y., Wang, L., & Wei, Q. (2014). A surface plasmon resonance assay coupled with a hybridization chain reaction for amplified detection of DNA and small molecules. *Chemical Communications, 50*(39), 5049–5052.

Liu, J., Cao, Z., & Lu, Y. (2009). Functional nucleic acid sensors. *Chemical Reviews, 109*(5), 1948.

Pagani, A., Villarreal, L., Capdevila, M., & Atrian, S. (2007). The saccharomyces cerevisiae crs5 metallothionein metal-binding abilities and its role in the response to zinc overload. *Molecular Microbiology, 63*(1), 256–269.

Shen, L., Chen, Z., Li, Y., He, S., Xie, S., Xu, X., ... Zhu, Z. (2008). Electrochemical DNAzyme sensor for lead based on amplification of DNA – Au Bio-Bar codes. *Analytical Chemistry, 80*(16), 6323–6328.

Soylak, M., Yilmaz, E., Ghaedi, M., & Montazerozohori, M. (2011). Solid phase extraction on multiwalled carbon nanotubes and flame atomic absorption spectrometry combination for determination of some metal ions in environmental and food samples. *Toxicological & Environmental Chemistry Reviews, 93*(5), 873–885.

Teller, C., Shimron, S., & Willner, I. (2009). Aptamer−DNAzyme hairpins for amplified biosensing. *Analytical Chemistry, 81*(21), 9114–9119.

Tian, L., & Yi, L. (2012). *Metal ion-dependent DNAzymes and their applications as biosensors.* Springer Netherlands.

Townsend, A. T., Miller, K. A., Mclean, S., & Aldous, S. (1998). The determination of copper, zinc, cadmium and lead in urine by high resolution ICP-MS. *Journal of Analytical Atomic Spectrometry, 13*(11), 1213–1219.

Travascio, P., Li, Y., & Sen, D. (1998). DNA-enhanced peroxidase activity of a DNA-aptamer-hemin complex. *Chemistry & Biology, 5*(9), 505–517.

Vashist, S. K., Schneider, E. M., Lam, E., Hrapovic, S., & Luong, J. H. (2014). One-step antibody immobilization-based rapid and highly-sensitive sandwich ELISA procedure for potential in vitro diagnostics. *Scientific Reports, 4*, 4407.

Walker, G. T., Fraiser, M. S., Schram, J. L., Little, M. C., Nadeau, J. G., & Malinowski, D. P. (1992). Strand displacement amplification–an isothermal, in vitro DNA amplification technique. *Nucleic Acids Research, 20*(7), 1691–1696.

Wang, C., Dong, X., Liu, Q., & Wang, K. (2015). Label-free colorimetric aptasensor for sensitive detection of ochratoxin A utilizing hybridization chain reaction. *Analytica Chimica Acta, 860*, 83–88.

Wu, C. S., Khaing Oo, M. K., & Fan, X. (2010). Highly sensitive multiplexed heavy metal detection using quantum-dot-labeled DNAzymes. *ACS Nano, 4*(10), 5897–5904.

Xiao, Y., Pavlov, V., Niazov, T., Dishon, A., Kotler, M., & Willner, I. (2005). Catalytic beacons for the detection of DNA and telomerase activity. *Journal of the American Chemical Society, 126*(24), 7430–7431.

Yang, J., Dou, B., Yuan, R., & Xiang, Y. (2016). Proximity binding and metal ion-dependent DNAzyme cyclic amplification-integrated aptasensor for label-free and sensitive electrochemical detection of thrombin. *Analytical Chemistry, 88*(16), 8218–8223.

Yin, B. C., Ye, B. C., Tan, W., Wang, H., & Xie, C. C. (2009). An allosteric dual-DNAzyme unimolecular probe for colorimetric detection of Copper(II). *Journal of the American Chemical Society, 131*(41), 14624.

Yin, B. C., Zuo, P., Huo, H., Zhong, X., & Ye, B. C. (2010). DNAzyme self-assembled gold nanoparticles for determination of metal ions using fluorescence anisotropy assay. *Analytical Biochemistry, 401*(1), 47–52.

Yin, H. S., Li, B. C., Zhou, Y. L., Wang, H. Y., Wang, M. H., & Ai, S. Y. (2017). Signal-on fluorescence biosensor for microRNA-21 detection based on DNA strand displacement reaction and Mg2+-dependent DNAzyme cleavage. *Biosensors & Bioelectronics, 96*, 106–112.

Zhang, B., Liu, B., Tang, D., Niessner, R., Chen, G., & Knopp, D. (2012). DNA-based hybridization chain reaction for amplified bioelectronic signal and ultrasensitive detection of proteins. *Analytical Chemistry, 84*(12), 5392.

Zhou, L. Y., Xin, G. S., & Pu, X. Y. (2012). Determination of microelements from different types of grass in the habitat of Przewalski's Gazelle by sealed microwave digestion ICP-AES. *Spectroscopy & Spectral Analysis, 32*(4), 1103–1105.

Zhu, G., & Zhang, C. Y. (2014). Functional nucleic acid-based sensors for heavy metal ion assays. *Analyst, 139*(24), 6326–6342.

Zhuang, J., Fu, L., Xu, M., Zhou, Q., Chen, G., & Tang, D. (2013). DNAzyme-based magneto-controlled electronic switch for picomolar detection of lead (II) coupling with DNA-based hybridization chain reaction. *Biosensors & Bioelectronics, 45*(2), 52–57.